

NEW CONSTRAINTS ON SURFACE DEBRIS LAYER COMPOSITION FOR MARTIAN MID-LATITUDE GLACIERS FROM SHARAD AND HIRISE E. I. Petersen¹, J. W. Holt¹, J. S. Levy¹, and T. A. Goudge² ¹Institute for Geophysics, University of Texas at Austin, Austin TX (eric.petersen@utexas.edu), ²Jackson School of Geosciences, University of Texas at Austin

Introduction: Debris-covered glaciers (DCGs) are abundant in the northern and southern mid-latitudes of Mars [1]. DCG are composed of relatively pure glacial ice under a debris cover 1-10m thick [2,3]. The debris layer has been hypothesized to be composed of headwall-derived talus, a dust-rich lag deposit, and/or a subsequent ice-rich mantle [4]. The composition is an important parameter for decoding the climate history recorded in DCG as well as assessing DCG as a water resource for human exploration. We show how geophysical analysis of existing data leads to constraints on the bulk composition of the surface debris.

Many but not all DCG exhibit basal reflectors in MRO Shallow Radar (SHARAD) sounding data [2,3]. In the dichotomy boundary region of Deuteronilus Mensae some DCG exhibit weak reflectors (Sites B & D, Fig. 2) or no reflectors at all (Site C, Fig. 1,2). In this work, which focuses on 4 DCG complexes in Deuteronilus Mensae, we show that variable surface roughness is sufficient to explain whether or not basal reflectors are observed. Furthermore, this work leads to constraints on the electric properties of the surface debris.

Methods: SHARAD Reflection Powers: We extracted SHARAD reflection powers for observed surface and subsurface reflections, as well as for non-detections (signal-free segments under DCG exhibiting no subsurface reflections). The reflection powers for the non-detections are used as a proxy for the effective noise floor for SHARAD data in this study.

A simple parametrization of the englacial radar volume attenuation was achieved by applying a linear regression to the observed subsurface signal power as a function of the thickness of the DCG deposit. The slope from this regression can be prescribed to correct SHARAD values for variable thickness of DCG.

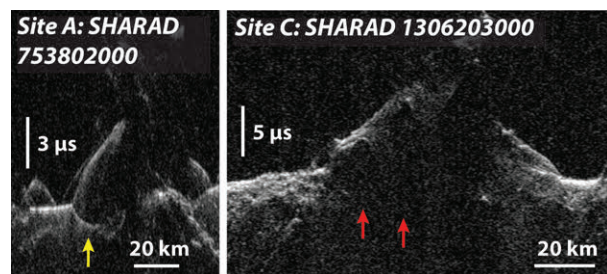


Figure 1: Example SHARAD radargrams for Site A (detection of subsurface signal) and Site C (non-detection of subsurface signal).

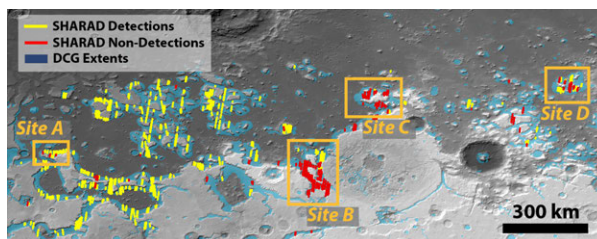


Figure 2: MOLA-derived map of Deuteronilus Mensae with confirmed detections and non-detections of DCG basal reflectors mapped. Selected DCG, designated Sites A, B, C, and D, are highlighted in orange boxes.

HiRISE DTM Surface Roughness: At least one HiRISE stereo pair is available for each of the study sites examined. We produced DTMs for each stereo pair using the Ames Stereo Pipeline [5,6], giving reliable results for the topography of features on the tens of meters scale. Roughness height deviation is produced by subtracting the mean elevation in a surrounding 50 meter wide square cell from each DTM pixel.

We used the roughness height values to calculate the expected transmission losses in a subsurface return as it passes through the surface, following the methods of [7]:

$$\sigma_\phi = \frac{4\pi\sigma_h}{\lambda}(\sqrt{\epsilon'} - 1)$$

$$\rho = e^{-\sigma_\phi^2} I_0^2\left(\frac{\sigma_\phi^2}{2}\right)$$

Where σ_ϕ is the rms phase delay in the SHARAD signal calculated from the roughness height σ_h , SHARAD wavelength λ (15 m), and the dielectric constant (real part) of the debris layer ϵ' . The signal loss ρ is then calculated from σ_ϕ using the zeroth-order Bessel function of the first kind, I_0 [7].

Results: SHARAD Reflection Powers: SHARAD's

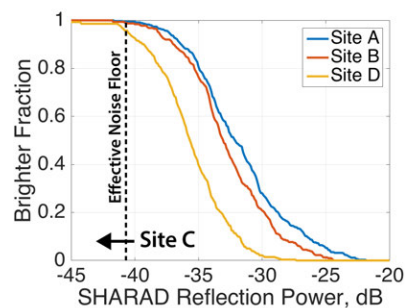


Figure 3: Subsurface reflection powers for study sites.

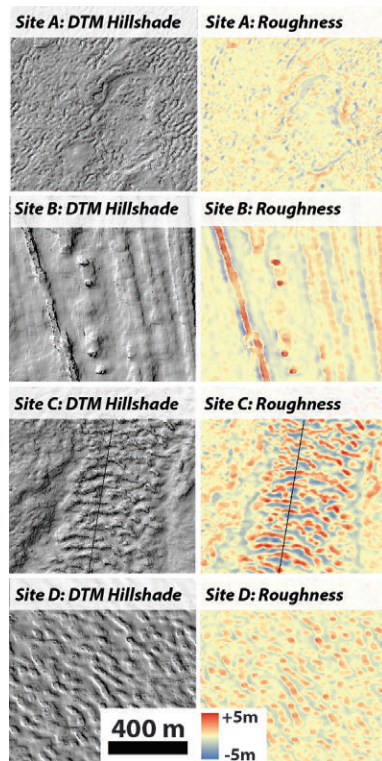


Figure 4: Hillshades and roughness values derived on fields of brain terrain in HiRISE DTMs produced for each of the sites. All images are at the same scale.

effective noise floor derived from non-detections is -40 dB. Attenuation values calculated at each of Sites A (-9 dB/km), B (-6 dB/km), and D (-4 dB/km) were low in comparison to values found by [2,3] (-9-18 dB/km), notably with the inclusion of Site B. Site B is an anomalously thick DCG deposit, exhibiting SHARAD reflections of comparable amplitude to the other sites fading out to noise level at a depth of 1.2 km. Site C exhibits no reflectors and thus is not included in this analysis.

From this analysis, we find the median values of subsurface reflectors at each of the sites to be: Site A = 31.8 ± 0.2 dB, Site B = -32.7 ± 0.2 dB, Site C < -40 dB, and Site D = -35.6 ± 0.2 dB.

HiRISE DTM Surface Roughness: Roughness values calculated for the HiRISE DTMs were similar between Sites A and B, with 7% of the surface at roughness values of >2 m. The DTM at Site C was much rougher, with 22% of values >2 m, while Site D exhibited an intermediate level of roughness with 15% of values >2m.

Signal loss curves as a function of the dielectric constant of the debris layer were normalized to Site A to compare with observed reflection powers. The differences between the median reflection powers at the sites can be satisfied by the signal loss curves assuming debris layer dielectric constants of 2.9-4.6 for Site B, >3.5 for

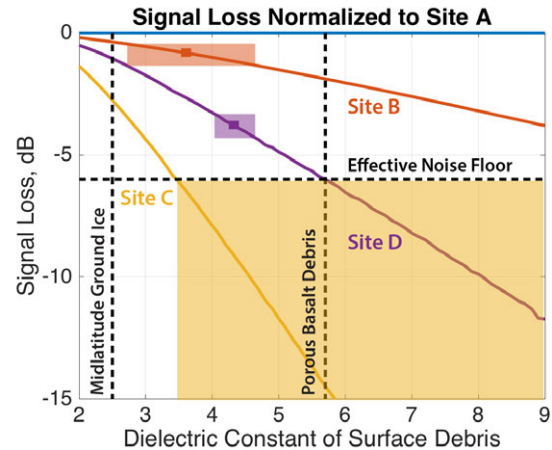


Figure 5: SHARAD signal loss as a function of the dielectric constant of the surface debris calculated from HiRISE DTMs on each of the study sites. All curves are normalized to Site A and the observed power reflection difference between each Site and Site A is shaded on each curve. These shaded regions overlap for $\epsilon' = 4.1-4.6$. Reference values are plotted for the dielectric constant of high porosity mid-latitude ground ice [8] and a dry basalt debris layer with 30% porosity.

Site C, and 4.1-4.6 for Site D. These values overlap for the range of $\epsilon' = 4.1-4.6$.

Discussion and Conclusions: We find that surface roughness is sufficient to explain the differences in SHARAD subsurface reflection power, provided a bulk dielectric constant for the surface debris layer of $\epsilon' = 4.1-4.6$ is assumed.

Using a power law mixing relation [8] with values of $\epsilon' = 8$ for basalt clasts, $\epsilon' = 3.15$ for water ice, and $\epsilon' = 1$ for air we estimated the debris layer composition. Rock with air-filled pore space requires porosities of 35-40% to reproduce $\epsilon' = 4.1-4.6$, while an air-free basalt-ice mix requires an ice content of 65-75%. Three-way mixtures are also feasible, including 15% air-filled pore-space in an equal mix of basalt and ice. Based on terrestrial analogs [9] we expect the debris layer porosity to be $\leq 33\%$, thus some degree of ice content appears likely.

Our geophysical analysis is thus consistent with a porous rocky debris layer with some ice content, likely sourced from subsequent ice mantling consistent with the model put forward by [4].

References: [1] Levy et al., 2014, JGR: Planets, 119(10), [2] Holt et al. (2008), Science, 322, 1235-1238. [3] Plaut et al. (2009), GRL, 36(2). [4] Baker and Head (2015), Icarus, 260, 269-288. [5] Broxton and Edwards (2008), LPSC 39, 2419, [6] Moratto et al. (2010), LPSC 41, 2364, [7] Schroeder et al. (2016), Geophysics, 81(1), [8] Bramson, et al. (2015), GRL, 42(16), 6566-6574, [9] Nichol森 and Benn (2013), ESPL 38, 490-501.